Report on self-directed joint research of MERIT

Visualization of electrode-reaction distribution in lithium-ion battery

Kosuke Kawai[1], Yohei Uemura[2]

[1]Department of Chemical System Engineering, Graduate School of Engineering, Yamada & Okubo Lab

[2]Department of Applied Physics, Graduate School of Engineering, Hasegawa & Arai Lab

Abstract

Visualizing distribution of electrode reactions in lithium-ion battery is important for rational design of the electrode structures. Herein, we tried to develop the visualization technique using visible lights as a probe of electrode reactions. A home-made lithium-ion battery which is suitable for optical observation in the atmosphere was demonstrated to operate by electrochemical measurements. However, no significant difference of modulation images for $Li_{1-x}CoO_2$ cathode after charge was observed because of negligible changes in its optical property through applying a voltage modulation.

Authors

Kosuke Kawai is engaging in the research of the energy storage materials for rechargeable batteries. In this study, K. Kawai is responsible for the synthesis of cathode materials and the fabrication of the electrochemical cell.

Yohei Uemura is engaging in the research of the material science in organic ferroelectrics. In this study, Y. Uemura is responsible for the measurement of modulation imaging.

1. Background

Performance improvement of lithium-ion battery needs rational design of electrode structures where electrode reactions occur efficiently. For this purpose, visualizing distribution of electrode reactions is of great importance because this technique helps in understanding of how electrodes reactions occur upon cycling.

Imaging technique with Raman spectroscopy has been widely used to analyze chemical state of electrode materials.[1–4] However, Raman spectroscopy is poor at element selectivity because Raman signal arises from vibration modes. Moreover, biproducts originating from oxidation/reduction decomposition of electrolyte accumulate on the surface of electrodes, obstructing the detection of electrode reactions. Such a situation makes it difficult to analyze stat-of-charge quantitatively because the signal of electrode reactions cannot be detected on systematic scale. Analytical methods using high-brightness X-ray and electron beam possess element selectivity with deep measurement depth (>10 nm) and high spatial resolution (<1 nm),[5–7] but take long time and large expenses. Therefore, it is necessary to develop a general and simple visualization method.

In this study, we focus on the modulation imaging technique using microscopic observation with visible light.[8,9] This technique detects changes in light transmittance/reflectance caused by applying external fields using difference image processing of optical images before and after the change (Fig. 1). Accumulating the difference images decreases noise level, enabling visualization of small differences (*ca*. 0.01%) in the optical image. During operation of lithium-ion battery, the modulation images may reflect changes in optical properties which corresponds to oxidation states (*e.g.*, state-of-charge) of electrode materials, and then visualize the distribution of electrode reactions. Moreover, change in absorbance is determined by wavelength of light and element. Thus, imaging with specific wavelength extracts signals from specific element. Using CMOS area sensors with millions of pixels realizes high-speed mapping and high spatial resolution (300–400 nm). Therefore, using modulation imaging technique would clarify how electrode reactions occurs during high-rate charge/discharge.

2. Purpose

Fabricating an electrochemical cell which is suitable for microscopic observation in the atmosphere and visualizing distribution of electrode reactions using modulation imaging technique with visible lights.

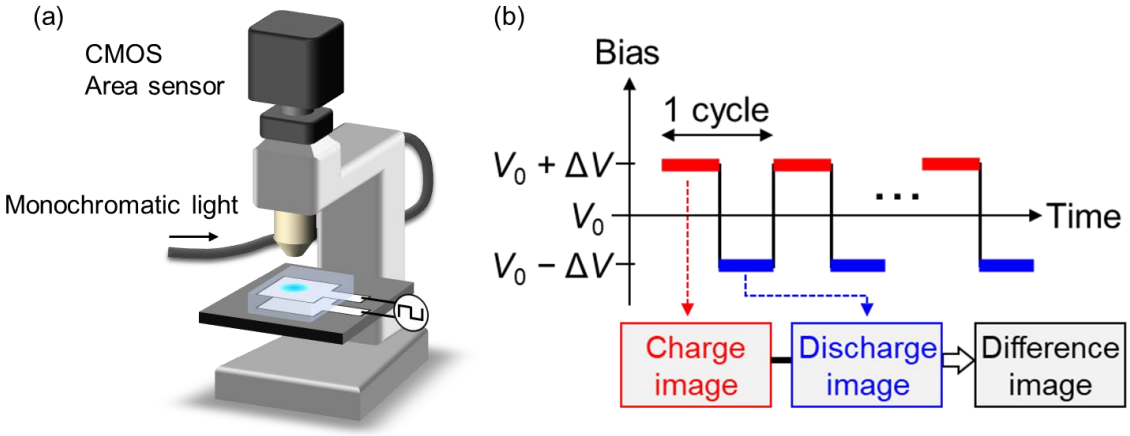

Fig. 1 Schematic illustrations of (a) a measurement instrument and (b) a modulation voltage for the modulation imaging technique.

3. Experimental

3.1 Fabrication of electrochemical cell

$LiCoO_2$ was synthesized by solid-state reaction. Li_2CO_3 (Kanto Chemical Co., Inc., purity: 99.0%) and CoO (FUJIFILM Wako Pure Chemical Corporation) in a molar ratio of 1:2 was mixed using a plenary ball-milling at 400 rpm for 12 h, and then heated at 800 °C for 12 h. Powder X-ray diffraction (XRD) pattern was measured using RINT TTR-III (Rigaku, copper as a radiation source). Crystal structure was drawn using VESTA.[10] $LiCoO_2$ and polyvinylidene fluoride (Kureha Corporation) in a weight ratio of 95:5 was mixed in N-methyl-2-pyrrolidone (Kanto Chemical Co., Inc., purity: >99.0%) using a magnetic stirrer. The slurry was mounted on SUS304 mesh (The Nilaco Corporation, wire diameter: 0.10 mm, mesh size: 0.149 mm) and dried at 80 °C for 1 h in air and then at 120 °C for 12 h under vacuum condition. The thickness of the electrode was *ca*. 0.10 mm. Anode was Li metal. Current collector of anode was nickel wires. Electrolyte was 1 mol dm^{-3} $LiPF_6$ ethylene carbonate:diethyl carbonate (KISHIDA CHEMICAL Co., Ltd., 1:1 vol%, battery grade). Separator was a glass fiber filter (Advantec, GB-100R), which was dried at 140 °C for 12 h under vacuum condition. Cell case was a transparent laminated package (SEISANNIPPONSHA Ltd., Lamizip®). Electrochemical cell was assembled in an Ar-filled glovebox. Cathode, separator, and anode were stacked for uniform electrode reactions. The package was sealed using heat clip and hot-melt adhesives for avoiding air contamination. Cyclic voltammetry at a scan rate of 0.2 mV/s and chronoamperometry were performed using the potentiostat/galvanostat, VMP3 (Bio-Logic Science Instruments Ltd.). Electrochemical measurements were started 12 h later after fabricating the cells to soak electrolyte into the electrode layer enough to realize uniform electrode reaction.

3.2 Modulation Imaging

In this study, the optical images were captured by an area image sensor at the charging and discharging processes, respectively, synchronized with the applied square-wave voltage bias. The difference of optical intensity in each pixel between captured images was collectively processed to obtain the modulation image, which shows the spatial distribution of the change in optical properties. The modulation image was repeatedly obtained and 16,384 images were accumulated to suppress the noise. In this way, the spatial distribution of $\Delta R/R$ was measured, where R is the reflectance at the reference voltage and ΔR is the difference between the reflectance at the charging and discharging processes. We used LED (Thorlabs, Inc., M455L4) as the light source, and the optical images were captured using a CMOS area image sensor (PCO AG, pco.edge 5.5). Based on the result that $Li_{1-x}CoO_2$ ($0 < x < 0.6$) operates in the potential range of 3.9–4.4 V (*vs.* Li/Li^+),[11] a modulation voltage of 1 V_{pp} (±0.5 V) was applied around the reference voltage of 3.9 V (*vs.* Li/Li^+). Namely, the optical images of the charging and the discharging process were captured at 4.4 V and 3.4 V, respectively. Since it is known that the electrode reaction occurs in the frequency range of about 1–1000 Hz,[12] we used 10 Hz as the frequency of the

square-wave voltage. The wavelength of the light used for modulation imaging was 455 nm, which has a relatively large wavelength dependence in the UV-vis absorption spectrum of $LiCoO_2$.[13] The magnification of the objective lens was 50x, which leads to the spatial resolution of about 300 nm. After the measurement of the modulation image in the initial state, 4.4 V (*vs.* Li/Li^+) was applied to the sample for 2 hours and then the modulation image was measured again to visualize the electrode reaction.

4. Results and discussions

The Bragg reflections of the powder XRD pattern of synthesized $LiCoO_2$ were indexed with a hexagonal lattice system (Fig. 2a). Lattice constants were a = 2.81541(3) Å and c = 14.0490(3) Å in a good agreement with the previous report.[11]

Pictures of the electrochemical cell are shown in Fig. 2b and 2c. None of electrolyte leakage, contamination of air bubbles, and discoloration of electrode and electrolyte was observed in the atmosphere under open circuit condition 24 h later after fabricating the cells. Cyclic voltammetry (Fig. 2d) showed the redox peaks at 3.9 V (*vs.* Li/Li^+).[11] Chronoamperometry (Fig. 2e) revealed that current density decayed to almost zero 1 h later after starting voltage application at 4.4 V (*vs.* Li/Li^+). Total capacity reached 175.6 mAh/g, which corresponds to oxidation of cobalt from +3.00 to +3.64, when 2 h passed. These results indicate that the home-made electrochemical cell operate correctly.

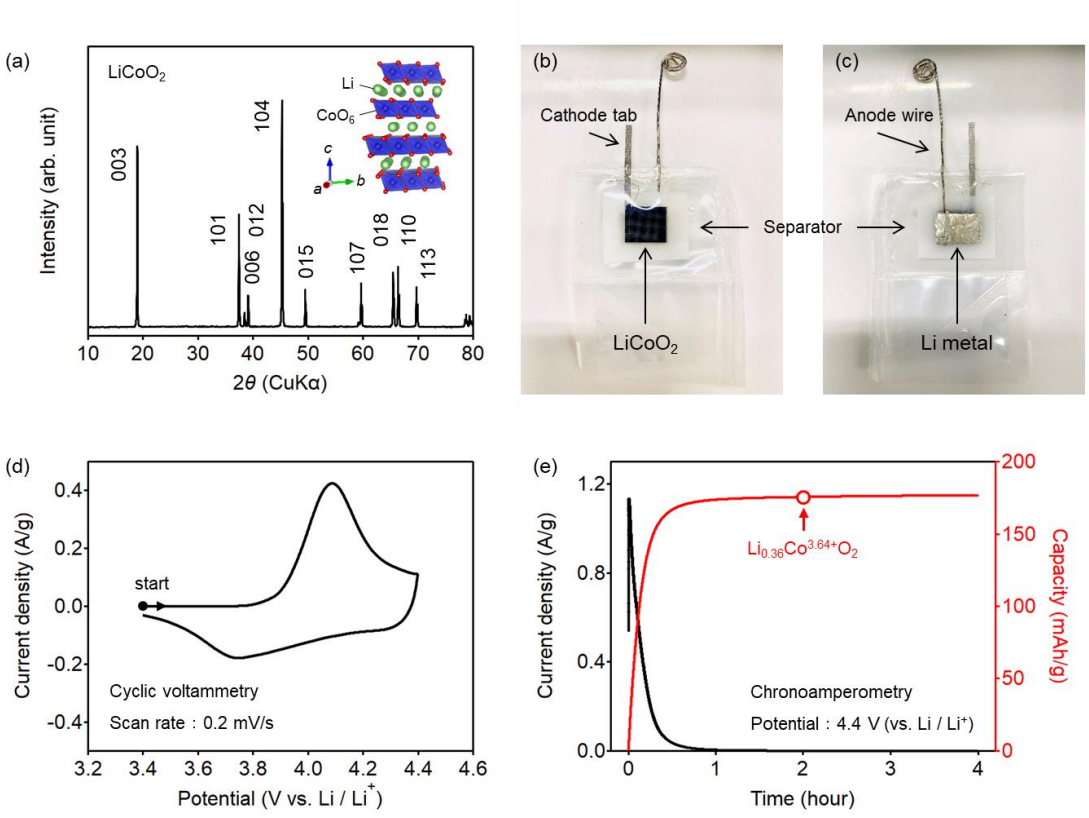

Fig. 2 (a) Powder XRD pattern of synthesized $LiCoO_2$, (b) cathode side and (c) anode side of the home-made electrochemical cell, (d) cyclic voltammogram, and (e) chronoamperogram.

Figure 3a shows the measurement system. Before charging, white spots with a diameter of *ca*. 3 μm, which are assumed to be $LiCoO_2$ particles, were observed in the optical image (upper left of Fig. 3b). The modulation image shows a uniform distribution of intensity (upper right of Fig. 3b). The intensity of signals $\Delta R/R$ was $<10^{-5}$, indicating that the optical image was unchanged through applying the modulation voltage. No significant difference in optical and modulation images were observed after keeping the voltage at 4.4 V (*vs*. Li/Li^+) for 2 h (lower left and right of Fig. 3b).

Contrary to our expectations, change of absorbance/reflectance after charge would be so small that the intensity was below the lower detection limit of modulation imaging in this measurement (frequency of voltage modulation: 10 Hz, wavelength: 455 nm). Enough signal from electrode reactions would be detected under other measurement conditions. For example, more electrode reactions may occur with lower frequency, leading to greater change of absorbance/reflectance enough to be detected. However,

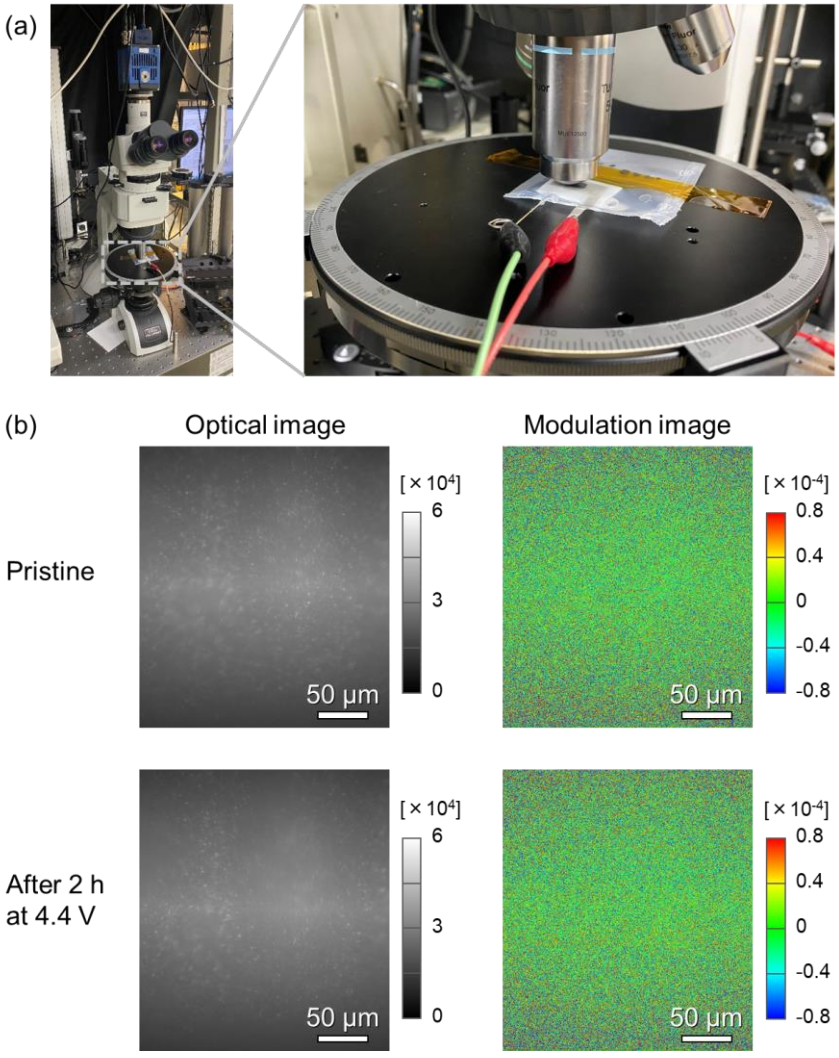

Fig. 3 (a) The picture of measurement system. Noises arising from vibration was suppressed by fixing the electrochemical cell on the observatory using adhesive tapes. (b) Surface of $Li_{1-x}CoO_2$ cathode. Median filtering was used for the modulation images to decrease noise level.

this condition is undesirable because lower frequency takes longer measurement time. Ultraviolet ray is more suitable as a probe of modulation images to visualize distribution of electrode reactions in $LiCo_{1-x}O_2$ cathode because absorption spectrum of $Li_{1-x}CoO_2$ in the ultraviolet region (<300 nm) changes greater than in the visible light region (>300 nm).

5. Conclusion

In this study, we tried to visualize distribution of the electrode reaction in $Li_{1-x}CoO_2$ cathode using the modulation imaging technique with visible lights. A home-made transparent electrochemical cell that is suitable for optical observation was demonstrated to operate as lithium-ion battery. However, modulation imaging for $Li_{1-x}CoO_2$ cathode could not visualize the distribution of the electrode reactions because of negligible change of optical property through applying a modulation voltage. Combination of electrode materials, frequency of voltage modulation, and wavelength is important for visualizing electrode-reaction distribution of lithium-ion battery using the modulation imaging technique.

Acknowledgement

We would like to express our gratitude to our supervisors, Prof. Atsuo Yamada and Prof. Tatsuo Hasegawa in the Graduate School of Engineering, for their great support and cooperation in carrying out this study. We would like to thank our sub-supervisors, Prof. Tatsuo Hasegawa and Prof. Masashi Kawasaki in the Graduate School of Engineering, for accepting the proposal of this study. We appreciate the MERIT program for giving us this valuable opportunity

References

[1] T. Gross *et al.*, *Rev. Sci. Instrum.* 84, 073109 (2013).

[2] T. Nishi *et al.*, *J. Electrochem. Soc.* 160 A1785–A1788 (2013).

[3] T. Gross & C. Hess, *J. Power Sources* 256, 220–225 (2014).

[4] E. Flores *et al.*, *Front. Energy Res.* 6, 82 (2019).

[5] Y. Gong *et al.*, *J. Am. Chem. Soc.* 139, 4274–4277 (2017).

[6] Y. Xu *et al.*, *ACS Energy Lett.* 2, 1240–1245 (2017).

[7] F. Zhang *et al.*, *Nat. Commun.* 11, 3050 (2020).

[8] J. Tsutsumi *et al.*, *Org. Electron.* 25, 289–294 (2015).

[9] Y. Uemura *et al.*, *Phys. Rev. Applied* 11, 014046 (2019).

[10] K. Momma & F. Izumi, *J. Appl. Cryst.* 44, 1272–1276 (2011).

[11] K. Mizushima, *et al.*, *Mater. Res. Bull.* 15, 783–789 (1980).

[12] W. Zhang *et al.*, *ACS Appl. Mater. Interfaces* 10, 22226–22236 (2018).

[13] F. Khatun *et al.*, *J. Sci. Res.* 6, 217–231 (2014).